Environmental Modelling and Software 185 (2025) 106318

Contents lists available at ScienceDirect

Environmental Modelling and Software

journal homepage: www.elsevier.com/locate/envsoft

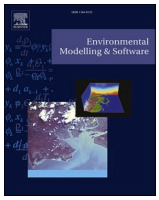

Land-N2N: An effective and efficient model for simulating the demand-driven changes in multifunctional lands

Yifan Gao, Changqing Song, Zhifeng Liu, Sijing Ye, Peichao Gao *

State Key Laboratory of Earth Surface Processes and Resource Ecology, Beijing Normal University, China

ARTICLE INFO

Keywords:
Multifunctional
Demand-driven
Land change simulation

ABSTRACT

Land is multifunctional. Among all land change models, the only model capable of modeling multifunctional land changes is the CLUMondo model. However, the CLUMondo model is ineffective and inefficient. In the study, we addressed the problems by improving the CLUMondo model through four strategies, resulting in the improved version named "Land-N2N". To evaluate the Land-N2N model, we designed six comparative experiments. In these experiments, we established the land systems using an upscaling approach based on Globeland30 data. Our finding shows that the effectiveness and efficiency of the Land-N2N model are better than the CLUMondo model. Specifically, the effectiveness of the Land-N2N model improved by 36% when measured with Kappa and by 377% when measured with Figure of Merit (FoM). Additionally, the efficiency of the Land-N2N model increased by 80%. The utility of the Land-N2N model lies in its ability to offer scientific solutions for land management by forecasting land changes.

1. Introduction

Land is multifunctional. It usually serves both social and ecological functions (Gu et al., 2022; Peng et al., 2017; Vreeker et al., 2004). These functions are not independent (Scherzinger et al., 2024) and collectively reflect both the characteristics of the land and extensive interactions between humans and nature. For example, in addition to the fundamental function of cropland, food production, cropland also provides functions such as social security, ecosystem conservation, and cultural heritage (Peng et al., 2017; Qian et al., 2020a). The multifunctionality perspective allows for a more comprehensive assessment of the impacts of land changes, helping decision-makers implement more effective land management (Scherzinger et al., 2024).

Global attention and research on multifunctional lands are gradually increasing. The concept of multifunctional originated in the agricultural sector (Liu et al., 2018, 2023). Recently, there has been a growing emphasis on multifunctional lands, which are now recognized as prevalent in various regions around the world. For example, Qian et al. (2020a) traded off synergy relationships of multifunctional cultivated land by analyzing the spatiotemporal distribution characteristics in Shenyang City, China. Gulickx et al. (2013) mapped the multifunctional landscape services of the Netherlands. Rallings et al. (2019) analyzed trade-offs and synergy of multifunctions in agriculture landscapes in Lower Fraser Valley, Canada.

However, when modeling land changes, we typically assume that land is unifunctional, which limits the ability to simulate multifunctional land change. These models do not support the assumption of multiple functions for a single land type because these models only allow land to serve one function, namely its area. The issue exists in many land change models, such as Conversion of Land Use and its Effects at Small regional extent (CLUE-S) (Verburg et al., 2002), the Future Land Use Simulation Model (FLUS model) (Li et al., 2017; Liu et al., 2017), and cellular automata model not driven by demands (Xing et al., 2020; Zhai et al., 2020).

Unifunctional land change simulations face three key challenges when forecasting future land changes. Specifically, the unifunctional land change models can be categorized into two categories, namely models driven by demands and models not driven by demands. First, in terms of the models not driven by demands, the challenge lies in the unclear definition of time points for the forecasting results. As a result, these models are rarely applied to land management decisions and are more commonly to explore the mechanisms of the models (Li et al., 2024; Qian et al., 2020b). Second, in terms of the models driven by demands, the challenge lies in how to scientifically set future demands. One solution to the challenge is to couple land change simulation models with other models, such as the system dynamic models (Liu et al., 2017)

* Corresponding author.
E-mail address: gaopc@bnu.edu.cn (P. Gao).

https://doi.org/10.1016/j.envsoft.2025.106318
Received 27 July 2024; Received in revised form 11 November 2024; Accepted 7 January 2025
Available online 7 January 2025

and integrated assessment models (Dong et al., 2018). However, the difficulty of coupling integrated assessment models arises from the divergence in the concept of land types between land data and integrated assessment models (Dong et al., 2018). Third, compared to multifunctional land change simulations, unifunctional land change simulation models struggle to effectively support land management. These models only can establish the relationship between land types and their corresponding areas. However, there is significant gap between land areas and human demands, as preserving land areas does not necessarily maintain their functions.

To the best of our knowledge, CLUMondo (van Asselen and Verburg, 2012) is the only demand-driven model that enables the assumption of land multiple functions but the CLUMondo model is ineffective and inefficient. Specifically, CLUMondo supports the assumption of many-to-many supply–demand relationships. For example, van Asselen and Verburg (2013) simulated the global land changes by defining four demands and 30 different land types. These four demands are crop production, livestock for bovines, goats, and sheep, livestock for pigs and poultry, and built-up areas.

In the study, we addressed the problems that the CLUMondo model is inefficient and ineffective by improving the CLUMondo through four strategies. First, we proposed using random forest regression models instead of Logistic regression models. Second, we proposed an iteration mechanism that combines coarse-grained and fine-grained iterations. Third, we proposed a competitive advantage method. The three strategies aim to increase the effectiveness. Fourth, we proposed a traversing strategy to decrease the time of simulation. We demonstrated the effectiveness and efficiency of Land-N2N is better than CLUMondo through comparative experiments.

2. Principles and limitations of CLUMondo

Since the release of the CLUMondo model, it has been widely applied to the simulation of global and regional areas. For example, van Asselen and Verburg (2013) simulated global land system changes using the CLUMondo model from 2000 to 2040 under the OECD Environmental Outlook scenario. The results provided insights into the debate between land sparing versus land sharing. Wang et al. (2020) evaluated the ecological protection effects by simulating the land use changes in Nanchang City from 2015 to 2040 under three development scenarios. Zhu et al. (2020) explored the land use changes of Horqin Sandy Land from 2015 to 2025 under three scenarios using the CLUMondo model to investigate the net primary productivity, crop production and wind protection, and sand fixation through a Bayesian belief network.

The principle of the CLUMondo model is to change land types according to transition rules that respond to changes in all demands through several iterations (Van Vliet and Verburg, 2018). At the end of each iteration, the CLUMondo model calculates the differences between the supplies and demands until the differences meet the conditions. The key characteristic of the CLUMondo model is its ability to establish many-to-many relationships between land types and demands (Van Vliet and Verburg, 2018). Additionally, the demands in CLUMondo can be defined in terms of land type areas or any quantifiable functions served by land, such as population, crop, and livestock (van Asselen and Verburg, 2012).

In each iteration, the transition rules of the CLUMondo model consist of transition potential and restricted conditions. Transition potential refers to the possibility of each cell changing to any land type, and the restricted conditions specify regions where cells cannot change and which land types are not allowed. Transition potential is determined by neighborhood effect, local suitability, competitive advantage, and resistance (Van Vliet and Verburg, 2018). Wherein, the neighborhood effect refers to the effect of neighboring cells on the center cell. Local suitability refers to the possibility of each cell changing to all land types, driven by nature and social factors. Notably, local suitability is the only spatial parameter of the CLUMondo model. Competitive advantage determines whether each land type should increase or decrease to meet demands. Resistance reflects the difficulty of changing each land type to other types. The restricted conditions consist of restricted spatial areas and restrictions between different land types.

Although CLUMondo enables land multifunctionality, the CLUMondo model is ineffective and inefficient. The ineffectiveness is reflected in the low accuracy of evaluating the CLUMondo model. The inefficiency is evident in the long simulation times required. The low effectiveness is likely due to the use of the Logistic regression model for calculating local suitability in the CLUMondo model. Several studies have shown that the performance of the Logistic regression model is worse than other regression models (Gao et al., 2023a; Lv et al., 2021). The low efficiency stems from the unnecessary determinations within the model through the theoretical analysis, which increases simulation time. Specifically, the CLUMondo model determines whether the land type of each cell, including NoData cells, will change in each iteration. NoData cells represent areas outside the study areas that will never undergo any changes. Since study areas are typically not rectangular, land data often contains many NoData cells. If the model needs to determine all cells during each iteration, it significantly reduces the simulation efficiency.

Based on the background, we proposed three methods to improve effectiveness and a traversing strategy to improve efficiency. The improved version, named "Land-N2N," operates independently of the CLUMondo model. When using the Land-N2N model, we do not need to run the CLUMondo model. To evaluate the effectiveness and efficiency of Land-N2N, we selected three study areas and designed comparative experiments. In addition, we demonstrated the importance of each improvement.

3. Land-N2N model

In the Land-N2N model, we proposed four strategies to improve the CLUMondo model. Three of these strategies aim to enhance the effectiveness of the CLUMondo, and one aims to improve efficiency. Technically, we implemented the Land-N2N model in C++ for three reasons. First, C++ is a compiled language for its fast execution speed. Second, since the CLUMondo model is also written in C++, we were able to use its source code of the CLUMondo model to facilitate the implementation of the Land-N2N model. Third, C++ is widely used in spatial analysis and environmental modeling. For example, the Global Change Assessment Model (GCAM) and CLUE-S model are implemented using C++.

3.1. Using a random forest regression model to calculate the local suitability

We proposed using the random forest regression model instead of the Logistic regression model to calculate the local suitability. The random forest model is a machine learning algorithm that can be applied for both classification and regression (Breiman, 2001; Wang et al., 2024). A random forest model consists of multiple decision trees (Belgiu and Drăguţ, 2016; Liang et al., 2021), which is why it is referred to as the “forest”. The “random” of the model is reflected in its approach to selecting features and samples. Specifically, each decision tree randomly selects a subset of features to build the nodes. During training, each decision tree is trained using samples selected through the bootstrap sampling method.

In the Land-N2N model, we established the relationships between driving factors and land type changes using the random forest regression model. According to the relationships we have established, we calculated the probability of changing to each land type for every cell (Eq. (1)). Before training the random forest regression model for changed land type *j*, we need to prepare samples. All samples can be categorized into positive and negative samples. Each sample consists of a label and a set of driving factors. The label is determined by comparing land data from two different periods. If the land type of a cell is changed to other

land types to j between the two periods, the land type j and the corresponding series of driving factors are composed of a positive sample. Otherwise, the other cells and the corresponding series of driving factors are composed of negative samples.

$$P\_loc_{c,j} = RF\left(X_{1,c},\ X_{2,c},\ \ldots, X_{m,c}\right) \tag{1}$$

Wherein, $X_{1,c},\ X_{2,c},\ \ldots, X_{m,c}$ are the driving factors of cell c.

3.2. Combining finer-grained iteration mechanism

In the Land-N2N model, we proposed an iteration mechanism that combines both coarser-grained iterations and finer-grained iterations to generate simulation results (Fig. 1). In the Land-N2N simulation process, several coarser-grained iterations are conducted initially. If the Land-N2N model does not produce the simulation results after several coarser-grained iterations, then the finer-grained iteration will be conducted.

The coarser-grained and finer-grained iterations in the Land-N2N model change both the land type of one or more cells and calculate the difference between supplies and demands to assess whether supply–demand balance has been achieved. The difference between coarser-grained iterations and finer-grained iterations lies in the scale of changing cells. Specifically, the coarser-grained iterations aim to quickly reduce the differences between supplies and demands. In a coarser-grained iteration, Land-N2N will change all of the cells that can be changed according to the transition rules. After each coarser-grained iteration ends, the model assesses whether supply–demand balance has been achieved. In finer-grained iterations, cells are changed individually one by one. After the land type of one cell is changed, the Land-N2N model immediately calculates whether supply-demand balance has been achieved.

3.3. Competitive advantage method

In the Land-N2N model, we developed a competitive advantage method by directly using supply capacities instead of conversion orders. Specifically, supply capacities refer to the quantitative value of each land type in serving each demand, and conversion orders refer to the descending rank of land types based on their supply capacities. This competitive advantage method more accurately reflects how the areas of each land type decrease or increase to meet the demands. The competitive advantages are calculated using Eq. (2).

$$\begin{cases} P\_cmp_{\mathrm{T}(c,t,0),j,(t,i)} = \sum_d intertia_{d,(t,i)} \times \dfrac{CA_{\mathrm{T}(c,t,0),d} - CA_{j,d}}{\sum_j CA_{j,d}} \\ intertia_{d,(t,i)} = \begin{cases} 0 & i = 1 \\ intertia_{d,(t,i)} + \dfrac{Demand_{d,t} - Supply_{d,i-1}}{Speed_i} & i \geq 2 \end{cases} \\ Speed_i = \begin{cases} Seed & i = 1 \\ Speed_{i-1} + Step & i \geq 2 \end{cases} \end{cases} \tag{2}$$

Wherein, $P\_cmp_{\mathrm{T}(c,t,0),j,(t,i)}$ represents the competitive advantage for changing land type $\mathrm{T}(c,t,0)$ to land type j at i-th iteration in time t. $CA_{\mathrm{T}(c,t,0),d}$ and $CA_{j,d}$ respectively represent the supply capacity of land type $\mathrm{T}(c,t,0)$ and land type j to provide to d-th demand. $Demand_{d,t}$ represents the d-th demand at time t. $Supply_{d,i-1}$ represents the supplies provided by the land at the $i-1$-th iteration. $Speed_i$ represents an iteration parameter. $Seed$ represents the initial value of the iteration parameter. $Step$ represents the step size of the iteration parameter.

3.4. Traversing strategy

In Land-N2N, we proposed a useful traversing strategy in each iteration to reduce the time of the simulation. Specifically, in each iteration, the traversing strategy only determines the land types that are not classified as Nodata instead of all cells. This strategy is implemented by creating a list consisting that consists of row and column indices of all non-Nodata cells (Fig. 2).

4. Model evaluation

To evaluate the effectiveness and efficiency of the Land-N2N model, we designed comparative experiments. An important assumption underlying this evaluation is that if a land change model reliably simulates

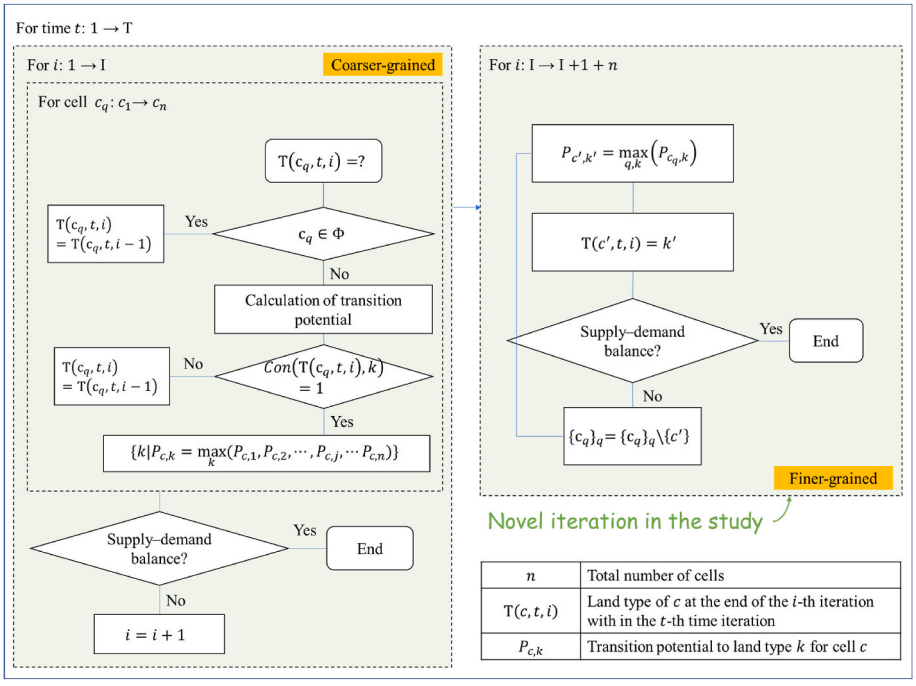

Fig. 1. The iteration mechanism.

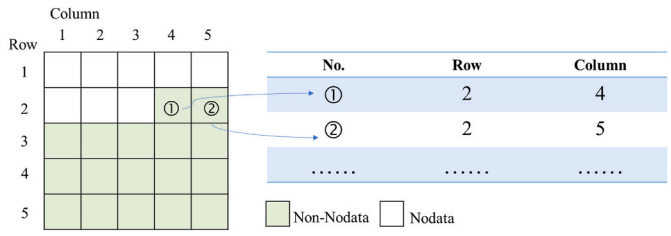

Fig. 2. The traversing strategy.

historical land changes, it can be considered reliable for forecasting future land changes (Jin et al., 2019). We selected three study areas and applied both the Land-N2N model and the CLUMondo model to simulate land changes from 2010 to 2020 in these areas. The effectiveness and efficiency of each model were then evaluated based on these simulations.

4.1. Materials

4.1.1. Selection of study areas

We employ four criteria to select study areas for a comprehensive evaluation of the effectiveness and efficiency of the Land-N2N model. First, multiple study areas are selected to reduce the impact of randomness. Second, the study areas are covered by different dominant land types. For example, one study area is primarily covered by natural vegetation, while the other study areas are covered by land types that are strongly relevant to human activities. Third, the study areas feature distinct landforms. Fourth, the study areas exhibit obvious land changes over a specific period to enhance the convincing of the evaluation.

According to the four criteria, we selected three study areas, namely Sichuan Province, Shaanxi Province, and Jiangsu Province (Fig. 3). The basic characteristics of the study areas are as follows.

- Sichuan Province

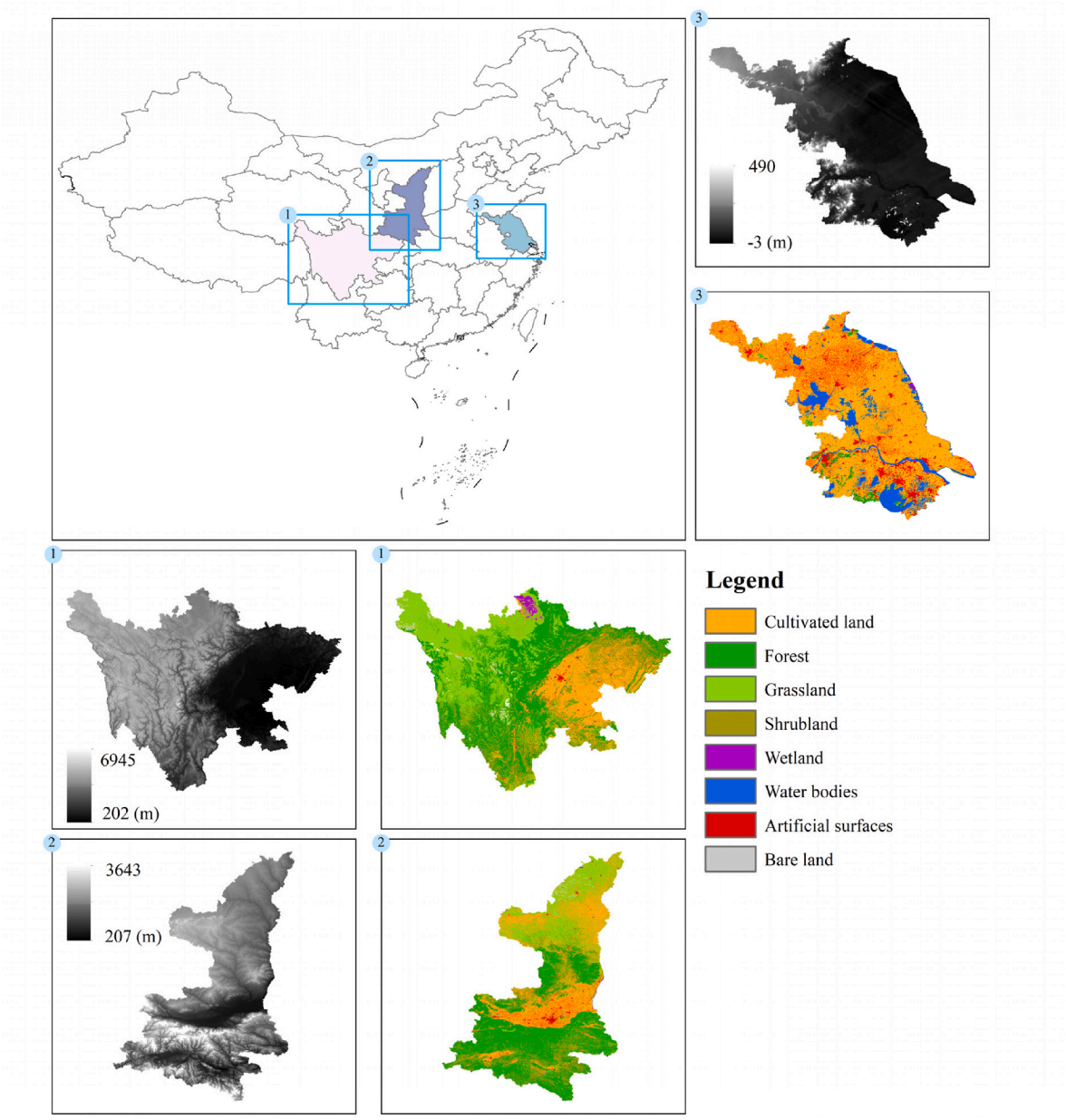

Fig. 3. Study areas.

Sichuan Province is located in the southwestern of China, covering an area of 486,000 km^2 (Gao et al., 2023b). The province features significant variations in terrain between east and west, with diverse topography. In the western of Sichuan Province, the landscape is dominated by plateaus and mountains, with elevations generally exceeding 4000 m. In contrast, the eastern region features basins and hills, with elevations ranging from 1000 m to 3000 m. According to the Globeland30 data in 2010, the dominant land cover types in Sichuan Province are forest (40.2%), grassland (30.6%), and cultivated land (23.9%).

- Shaanxi Province

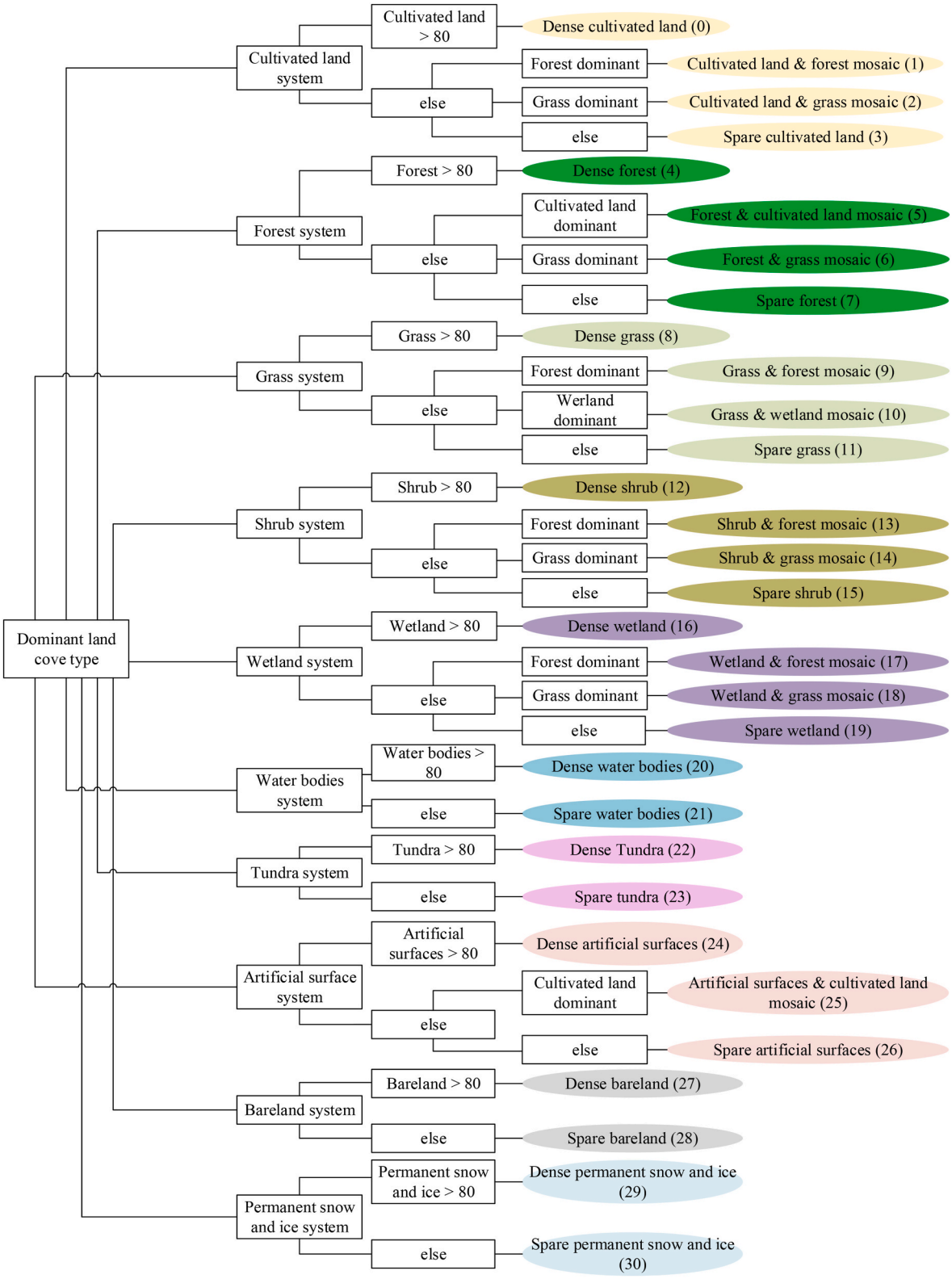

Fig. 4. Rules of establishing land system maps.

Shaanxi Province, located in the heartland of China along the middle reaches of the Yellow River, covers an area of 205,600 km^2. Shaanxi Province spans diverse terrain from north to south and can be divided into three main geomorphic regions: the Northern Shaanxi Plateau, Guanzhong Plain, and Qinba Mountainous. According to Globeland30 data in 2010, the dominant land cover types in Shaanxi Province are forest (44.6%), cultivated land (30.6%), and grassland (21.1%).

- Jiangsu Province

Jiangsu Province is located in eastern China, along the lower reaches of the Yangtze River and Huai River, covering an area of 107,200 km^2. Jiangsu Province is a major economic and commercial center in China. It is predominantly composed of alluvial plains, making it one of the flattest provinces in China. The dominant land cover types are cultivated land (70.9%), water bodies (13.0%), and artificial surfaces (12.9%).

4.1.2. Land system

We established land system maps in the study. Compared the traditional land use or land cover, land systems offer a more comprehensive representation of human demands and spatial configurations (Dou et al., 2021). Specifically, land systems can reflect the functions and patterns. Here, "functions" are closely related to human demands, and "patterns" refer to two concepts: components and configurations. Components reflect the fractions of different land types, and configurations can reflect the spatial structure of land types (Schmid et al., 2021; Van Vliet and Verburg, 2018).

In the study, we selected the Globeland30 dataset (Chen et al., 2015; Lv et al., 2025) to establish the land system maps. The Globeland30 dataset consists of three periods, namely 2000, 2010, and 2020. Globeland30 categorizes land into ten land cover types, namely cultivated land, forest, grassland, shrubland, wetland, water bodies, tundra, artificial surfaces, bare land, permanent snow and ice. The resolution of the Globeland30 dataset is 30 m.

We established the land system maps using an upscaling approach based on the Globeland30 dataset. Specifically, the process of establishing the land system map is to slide the Globeland30 dataset. In each sliding window, we first identify the dominant land cover type. If the fraction of the dominant land cover type exceeds the predefined threshold, we classify the land system type after upscaling as the dense type, such as "Dense cultivated land". If the fraction of the dominant land cover type is less than the threshold, we determine the land system type according to the dominant and suboptimal land cover type. For example, if the dominant land cover type is cultivated land (with a fraction below the threshold) and the suboptimal land cover type is forest, we define the land system type as "Cultivated & forest mosaic". If these conditions are not met, we define the land system type as spare types, such as "Spare cultivated land". The detailed rules for establishing the land system maps are shown in Fig. 4. We established land systems for each land cover type in Globeland30. These rules are based on the

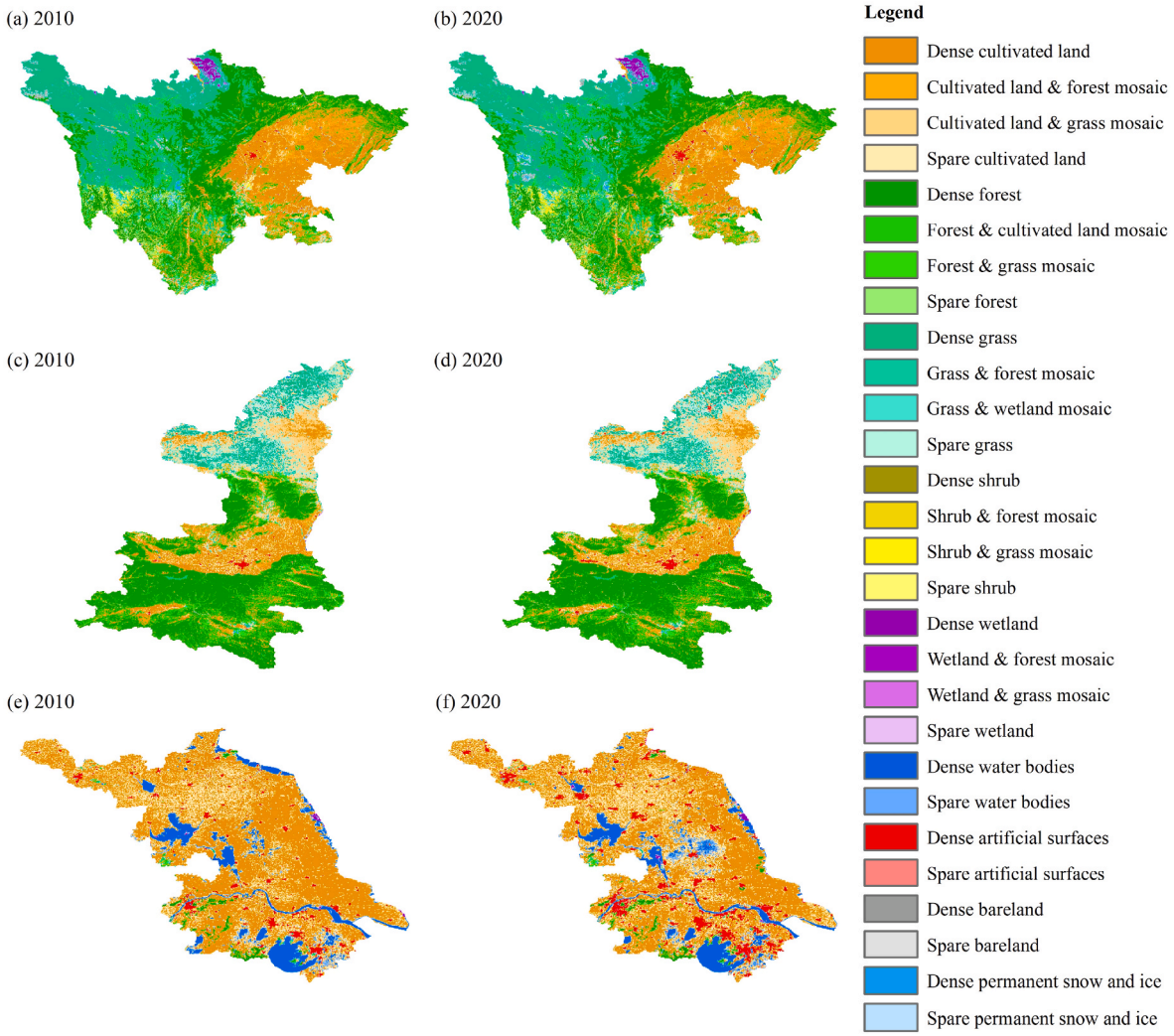

Fig. 5. Land system maps in study areas.

neighborhood relationships among land cover types. In the study, we specified the threshold as 80% and configured the size of the sliding windows to be 33 × 33. Notably, the threshold can be flexibly specified by users. After sliding, we established the 990 m resolution land system maps. Subsequently, we resampled the 990 m resolution land system maps into 1 km land system maps. The land system maps of the study areas are shown in Fig. 5.

4.1.3. Driving factors

The criterion for selecting driving factors is to comprehensively reflect the factors that drive land changes in each land type. In this study, we referred to the driving factors selected by Gao et al. (2023a). Specifically, we selected 54 driving factors, which were categorized into eight categories: soil, socioeconomic status, accessibility, agriculture and vegetation, terrain, climate, and livestock. Compared to the driving factors provided by Gao et al. (2023a), we removed the night light data. A detailed list of the driving factors is in supplementary materials. In this study, all driving factors were processed into the World_Cylindrical_Equal_Area coordinate system with 1 km resolution.

4.2. Methods

4.2.1. Design of comparative experiments

There are two objectives for comparative experiments. The first objective is to demonstrate that the Land-N2N model is more effective than the CLUMondo model. To underscore the significance of each improvement, we also evaluated how each improved method improves its effectiveness. The second objective is to demonstrate the efficiency of the Land-N2N model is better than the CLUMondo model. However, due to the different principles of the two models, the two models would generate different results. Therefore, it does not make sense to directly compare the simulation time of the two models. In the study, we designed an alternative solution to compare the efficiency by comparing the simulation time between the Land-N2N model and Land-N2N without the traversing strategy we proposed.

We designed six experiments to evaluate the effectiveness and efficiency of Land-N2N, as shown in Table 1. In these six experiments, comparing “Land-N2N” to “CLUMondo” aims to demonstrate the better effectiveness of Land-N2N. Comparing “Land-N2N” to “Experiment D” aims to demonstrate the better efficiency of Land-N2N. In addition, comparing “Experiment A”-“Experiment C” with “Land-N2N” aims to demonstrate the significance of random forest regression, the comparative advantages, and the iteration mechanism in improving effectiveness.

4.2.2. Demands

We establish five demands for each study area, namely the areas of cropland, forest, grassland, shrubland, and artificial surfaces in Globeland30 (Table 2). It is noted that the demands refer to the areas of the land cover types, not the area of land system types. The reason for establishing these five demands is that they account for 97.6%、96.7% and 86.7%, respectively, of the area of the entire region in study areas. Additionally, the five demands represent primary natural vegetation and artificial surfaces. Notably, when simulating the land change in Jiangsu Province, we did not set the areas of shrubland as a demand because the areas of shrubland are too small.

Table 1
Comparing experiments.

Experiment	Random forest	Comparative advantages	Iteration mechanism	Traversing strategy
Land-N2N	✓	✓	✓	✓
CLUMondo	×	×	×	×
Experiment A	×	✓	✓	✓
Experiment B	✓	×	✓	✓
Experiment C	✓	✓	×	✓
Experiment D	✓	✓	✓	×

4.2.3. Definition of multifunctions for each land

In the study, we emphasized the multifunctional lands through the many-to-many relationships between land types and demands. Specifically, we calculated the supply capacity for each demand within each land system type by overlapping the land system map and land cover map. The supply capacities were quantified by calculating the average areas of the land cover type corresponding to each demand in each land system type. For example, to calculate the supply capacity of “Dense cultivated land” for the area of cultivated land, we need to calculate the average areas of cultivated land in all “Dense cultivated land” cells. The steps of calculating supply capacities consist of three steps. First, we calculated the areas of five land cover types (30 m resolution)—cultivated land, forest, grassland, shrubland, and artificial surfaces—for each 990 m land system cell. Second, in terms of each land system type, we calculated the average areas of these five land cover types. Third, we calculated the average areas of five land cover types at 1 km resolution. The supply results for the three study areas are provided in the supplementary material. Here, we only provided the supply capacities in Sichuan Province (Table 3). The results showed that each land system type served more than one demand in three study areas.

4.2.4. Other settings

- Random forest regression

In the Land-N2N model, we calculated the local suitability using a random forest regression model. To better organize the Land-N2N model, we separated the calculation of suitability from the core model. The random forest regression was implemented using the scikit-learn package. During the training process, we regarded the land system map at the beginning of the simulation as the land system map for sampling (Time 1), and we regarded the land system map at the end of the evaluation as the land system map for sampling (Time 2). Additionally, if the number of positive samples of one land type is less than 10, we will not execute the regression for that land type.

- Logistic regression

In the CLUMondo model, we calculated the local suitability through Logistic regression. The CLUMondo model does not consist of a module for calculating local suitability. In the study, we implemented Logistic regression using Statistical Product and Service Solutions (SPSS). We selected a stepwise regression approach in our regression.

- Restrictions between different land types

The restrictions between different land types are calculated through the cell-by-cell analysis of the historical land system maps from 2010 to 2020. If any two land types existed conversion from 2010 to 2020, we allowed these two land types to be converted in the simulation.

- Resistance

We calculated the resistance by calculating the fractions of a land system type that remained unchanged from 2010 to 2020.

4.3. Evaluation metrics

4.3.1. Metrics for evaluating effectiveness

To comprehensively evaluate the effectiveness of Land-N2N, we

Table 2
Demands in the three study areas (Unit: km^2).

Study areas	Year	Cultivated land	Forest	Grassland	Shrubland	Artificial surfaces
Sichuan Province	2010	116,848.3	196,017.5	149,378.4	9720.4	2414.9
	2020	113,116.1	194,637.2	148,022.0	9771.0	5871.8
Shaanxi Province	2010	62,948.2	91,581.3	43,342.4	766.3	4476.1
	2020	61,949.5	91,326.2	42,448.1	786.4	6648.8
Jiangsu Province	2010	72,266.1	2102.4	723.0	2.6	13,151.4
	2020	64,396.1	2436.3	662.1	1.5	20,059.5

Table 3
The supply capacities in Sichuan Province.

Land system	Supply capacity				
	Cultivated land	Forest	Grassland	Shrubland	Artificial surfaces
Dense cultivated land	0.961	0.031	0.013	0.001	0.009
Cultivated land & forest mosaic	0.637	0.312	0.059	0.004	0.002
Cultivated land & grass mosaic	0.625	0.114	0.261	0.009	0.003
Spare cultivated land	0.640	0.045	0.040	0.047	0.096
Dense forest	0.016	0.974	0.022	0.008	0.000
Forest & cultivated land mosaic	0.320	0.633	0.055	0.008	0.001
Forest & grass mosaic	0.034	0.640	0.317	0.027	0.000
Spare forest	0.018	0.638	0.086	0.225	0.004
Dense grass	0.001	0.017	0.998	0.001	0.000
Grass & forest mosaic	0.021	0.337	0.636	0.022	0.000
Grass & wetland mosaic	0.002	0.001	0.675	0.000	0.002
Spare grass	0.138	0.090	0.596	0.105	0.005
Dense shrub	0.008	0.047	0.078	0.887	0.000
Shrub & forest mosaic	0.013	0.333	0.139	0.529	0.000
Shrub & grass mosaic	0.015	0.119	0.323	0.557	0.001
Spare shrub	0.283	0.087	0.107	0.496	0.010
Dense wetland	0.001	0.000	0.030	0.000	0.000
Wetland & forest mosaic	0.087	0.185	0.121	0.011	0.000
Wetland & grass mosaic	0.001	0.001	0.357	0.000	0.001
Spare wetland	0.194	0.016	0.048	0.004	0.021
Dense water	0.033	0.022	0.017	0.004	0.002
Spare water	0.238	0.110	0.067	0.012	0.025
Dense Tundra	0.000	0.000	0.000	0.000	0.000
Spare tundra	0.000	0.000	0.000	0.000	0.000
Dense artificial surfaces	0.037	0.003	0.005	0.001	0.965
Artificial surfaces & cultivated land mosaic	0.000	0.000	0.000	0.000	0.000
Spare artificial surfaces	0.081	0.092	0.125	0.035	0.567
Dense bare land	0.000	0.002	0.062	0.000	0.000
Spare bare land	0.003	0.031	0.321	0.005	0.000
Dense permanent snow and ice	0.000	0.030	0.025	0.003	0.000
Spare permanent snow and ice	0.000	0.198	0.172	0.040	0.000

selected two metrics from two perspectives, namely the Kappa coefficient (Cohen, 1960; Lin et al., 2020a) and FoM (Liu et al., 2017). Specifically, the Kappa coefficient evaluates the agreement between the simulation land system map and the actual land system map (van Vliet et al., 2011). The Kappa coefficient ranges from −1 to 1, with higher values indicating greater simulation accuracy. The FoM calculates the proportion of correctly changed cells relative to the total number of changed cells in the simulation to evaluate the accuracy of change (Zhang et al., 2023). The FoM ranges from 0 to 1, with higher values indicating greater simulation accuracy. The calculation formulas are shown in Eq. (3) and Eq. (4).

$$\text{Kappa} = \frac{p_0 - p_e}{1 - p_e} \tag{3}$$

$$\text{Fom} = \frac{\text{Hits}}{\text{Hits} + \text{Miss} + \text{False alarm} + \text{C}} \tag{4}$$

Here, p_0 represents the proportion of agreement between ground and simulated results through cell-by-cell. p_e represents the probability of chance agreement. False alarm represents the number of cells that remained unchanged in the ground land change but changed in the simulated land change. Hits represents the number of cells that changed in the ground land change and correctly changed in the simulated land change. Miss represents the number of cells that changed in the ground land change but did not change in the simulated land change. C represents the number of cells that changed in the ground land change but were incorrectly simulated as unchanged.

4.3.2. *Metrics for evaluating efficiency*

To evaluate the efficiency of Land-N2N, we recorded the simulation time of “Land-N2N” and “Experiment D”. To avoid the influence of devices and software environments on simulation, we ensured that both experiments were run on the same devices and within the same software environment.

Table 4
The evaluation results of effectiveness.

Study area	Experiment	Kappa coefficient	FoM
Sichuan Province	Land-N2N	89.48%	11.55%
	CLUMondo	76.14%	1.92%
	Experiment A	83.46%	1.42%
	Experiment B	–	–
	Experiment C	89.48%	11.55%
Shaanxi Province	Land-N2N	88.54%	22.45%
	CLUMondo	60.76%	4.19%
	Experiment A	–	–
	Experiment B	–	–
	Experiment C	–	–
Jiangsu Province	Land-N2N	65.59%	23.98%
	CLUMondo	45.66%	8.18%
	Experiment A	52.89%	6.49%
	Experiment B	62.67%	28.74%
	Experiment C	65.59%	23.98%

Note: “-” represents that the experiment does not produce the simulation results.

4.4. Results

The evaluation results of effectiveness are shown in Table 4. In three study areas, the Kappa coefficient and FoM in "Land-N2N" are better than "CLUMondo". Specifically, "Land-N2N" averaged a 35.63% improvement in the Kappa coefficient and a 377% improvement in the FoM improvement compared to "CLUMondo". These results demonstrated that the Land-N2N model is more effective than the CLUMondo model.

Notably, the results also showed that the three improvements are indispensable:

- Using random forest regressions instead of Logistic regressions significantly improved the accuracy of the simulations.

In the results of the Sichuan Province and Jiangsu Province, the Kappa coefficient improved by 7.21% and 24.01%, respectively, compared to "Experiment A". Similarly, the FoM improved by 713.38% and 269.49%, respectively.

- Using comparative advantage methods and iteration mechanisms contributed to the results of the Land-N2N model.

In Sichuan Province, "Experiment B" failed to produce the simulation results. And in Shaanxi Province, "Experiment C" failed to produce the simulation results. It should be noted that the same results of "Land-N2N" and "Experiment C" in Sichuan Province and Jiangsu Province occurred because the simulation results were produced without the opportunity to utilize the iteration mechanism.

The evaluation results of efficiency are shown in Table 5. On average, the efficiency was improved by 79.83 % in the three study areas, demonstrating that the traversing strategy significantly decreased the simulation time.

5. Discussion and conclusion

The contribution of the study lies in that we proposed a more effective and efficient model for simulating demand-driven changes in multifunctional lands by improving the CLUMondo through four strategies. To evaluate the effectiveness and efficiency of the Land-N2N model, we selected three study areas and designed comparative experiments. In three study areas, the Land-N2N model achieves higher simulation accuracy and takes less simulation time compared to the CLUMondo model. Higher model simulation accuracy can boost the confidence of policymakers in their decisions. The higher simulation accuracy has demonstrated that the effectiveness of the Land-N2N model is better than the CLUMondo model, especially in FoM. In particular, the Land-N2N model showed an average 377% improvement in FoM compared to CLUMondo. The reason for the improvement of FoM is that the random forest is a more suitable method for characterizing the relationships between land types and driving factors. Specifically, Logistic regression requires independent driving factors, but the driving factors are always not completely independent. In addition, we also demonstrated that the four improvements are indispensable.

It should be noted that no uncertainty exists in the Land-N2N model. If we prepare the same inputs for the Land-N2N model, we will get the same results. Some land change models incorporate random factors to account for unpredictable elements, such as the FLUS model (Liu et al., 2017) and the model proposed by Qian et al. (2020b). Specifically, the FLUS model incorporates random factors through roulette. The model proposed by Qian et al. (2020b) incorporates random factors by adding a stochastic number into transition potential. However, it remains uncertain whether these random factors can effectively reflect the unpredictable elements, which is why we do not incorporate random factors into the Land-N2N model.

Table 5
The evaluation results of efficiency.

Study area	Experiment	Simulation time (Unit: s)
Sichuan Province	Land-N2N	335
	Experiment D	708
Shaanxi Province	Land-N2N	2162
	Experiment D	3824
Jiangsu Province	Land-N2N	39
	Experiment D	55

The general utility of the Land-N2N model is to forecast the demand-driven changes in multifunctional land under various social and economic scenarios by generating future land system maps. These maps provide valuable insights for decision-makers by visualizing the probabilities of future land system changes. With these insights, decision-makers can develop more effective land management policies to promote regional or global sustainable development. Compared to the unifunctional land change models, the Land-N2N model can offer information about land intensity, density, or spatial configuration based on the land system maps used by users. In addition, the future land system maps can provide data for other research. For example, the future land system maps can be used as the basic data for the loss evaluations because of the sea level rise (Vousdoukas et al., 2023), terrestrial ecosystem carbon storage evaluation (Gao et al., 2023a; Wang et al., 2024), and flood risk analysis(Lin et al., 2020b).

The Land-N2N model still encounters the challenges. First, the first challenge is how to scientifically settle future demands. Demands are crucial in the Land-N2N model, as they influence the change trends of each land system type. However, the model cannot forecast future demands, which must be provided by users. Fortunately, there are existing solutions to address this challenge. A common solution to the challenge is to integrate the system dynamics models or integrated assessment models with the Land-N2N model (Liu et al., 2017; Wang et al., 2024). These models can provide scientific future demands, including population, areas of land types, and GDP. Second, another challenge is the assumption that supply capacities remain constant over time. But in reality, supply capacities are often changed dynamically over time due to factors such as technological advancements or environmental changes.

In future work, we aim to improve the Land-N2N model by improving the mechanisms and integrating the Land-N2N model with other models. First, we will strengthen the many-to-many supply–demand relationships by incorporating spatial heterogeneity. Second, we will integrate the Land-N2N model with the GCAM model. The GCAM model is designed to enhance our understanding of future water, energy, land, climate, and socioeconomic changes under various scenarios (Calvin et al., 2019). The GCAM model has been widely applied to explore the effects of different climate pledges and emission scenarios (Dong et al., 2018; Iyer et al., 2022). Integrating GCAM with the Land-N2N model can provide a more scientific solution for forecasting demands and examining the effect of land change on climate change.

CRediT authorship contribution statement

Yifan Gao: Writing – original draft, Software, Methodology, Investigation, Formal analysis, Data curation. **Changqing Song:** Writing – review & editing, Supervision, Project administration. **Zhifeng Liu:** Writing – review & editing, Methodology. **Sijing Ye:** Writing – review & editing, Resources. **Peichao Gao:** Writing – review & editing, Supervision, Methodology, Funding acquisition.

Software and data availability

The Land-N2N model and the source code for establishing land systems can be accessed at https://github.com/gaoyifan2021/Land-N2N-v1. In addition, we provide all data in comparative

experiments at https://doi.org/10.5281/zenodo.13079384.

Data availability

The data have been published at https://doi.org/10.5281/zenodo.13079384.

Declaration of competing interest

The authors declare that they have no known competing financial interests or personal relationships that could have appeared to influence the work reported in this paper.

Acknowledgments

This work has been supported by the National Natural Science Foundation of China (Grant Nos. 42271418 and 42230106).

Appendix A. Supplementary data

Supplementary data to this article can be found online at https://doi.org/10.1016/j.envsoft.2025.106318.

Data availability

We have shared the code at https://github.com/gaoyifan2021/Land-N2N-v1 and data at https://doi.org/10.5281/zenodo.13079384

References

Belgiu, M., Drăguţ, L., 2016. Random forest in remote sensing: a review of applications and future directions. ISPRS J. Photogrammetry Remote Sens. 114, 24–31. https://doi.org/10.1016/j.isprsjprs.2016.01.011.

Breiman, L., 2001. Random forests. Mach. Learn. 45 (1), 5–32. https://doi.org/10.1023/A:1010933404324.

Calvin, K., Patel, P., Clarke, L., Asrar, G., Bond-Lamberty, B., Cui, R.Y., Di Vittorio, A., Dorheim, K., Edmonds, J., Hartin, C., 2019. GCAM v5. 1: representing the linkages between energy, water, land, climate, and economic systems. Geosci. Model Dev. (GMD) 12 (2), 677–698. https://doi.org/10.5194/gmd-12-677-2019.

Chen, J., Chen, J., Liao, A., Cao, X., Chen, L., Chen, X., He, C., Han, G., Peng, S., Lu, M., 2015. Global land cover mapping at 30 m resolution: a POK-based operational approach. ISPRS J. Photogrammetry Remote Sens. 103, 7–27. https://doi.org/10.1016/j.isprsjprs.2014.09.002.

Cohen, J., 1960. A coefficient of agreement for nominal scales. Educ. Psychol. Meas. 20 (1), 37–46. https://doi.org/10.1177/001316446002000104.

Dong, N., You, L., Cai, W., Li, G., Lin, H., 2018. Land use projections in China under global socioeconomic and emission scenarios: utilizing a scenario-based land-use change assessment framework. Global Environ. Change 50, 164–177. https://doi.org/10.1016/j.gloenvcha.2018.04.001.

Dou, Y., Cosentino, F., Malek, Z., Maiorano, L., Thuiller, W., Verburg, P.H., 2021. A new European land systems representation accounting for landscape characteristics. Landsc. Ecol. 36, 2215–2234. https://doi.org/10.1007/s10980-021-01227-5.

Gao, P., Gao, Y., Ou, Y., McJeon, H., Zhang, X., Ye, S., Wang, Y., Song, C., 2023a. Fulfilling global climate pledges can lead to major increase in forest land on Tibetan Plateau. iScience 26 (4). https://doi.org/10.1016/j.isci.2023.106364.

Gao, P., Gao, Y., Zhang, X., Ye, S., Song, C., 2023b. CLUMondo-BNU for simulating land system changes based on many-to-many demand–supply relationships with adaptive conversion orders. Sci. Rep. 13 (1), 5559. https://doi.org/10.1038/s41598-023-31001-3.

Gu, X., Xu, D., Xu, M., Zhang, Z., 2022. Measuring residents' perceptions of multifunctional land use in peri-urban areas of three Chinese megacities: suggestions for governance from a demand perspective. Cities 126, 103703. https://doi.org/10.1016/j.cities.2022.103703.

Gulickx, M., Verburg, P., Stoorvogel, J., Kok, K., Veldkamp, A., 2013. Mapping landscape services: a case study in a multifunctional rural landscape in The Netherlands. Ecol. Indicat. 24, 273–283. https://doi.org/10.1016/j.ecolind.2012.07.005.

Iyer, G., Ou, Y., Edmonds, J., Fawcett, A.A., Hultman, N., McFarland, J., Fuhrman, J., Waldhoff, S., McJeon, H., 2022. Ratcheting of climate pledges needed to limit peak global warming. Nat. Clim. Change 1–7. https://doi.org/10.1038/s41558-022-01508-0.

Jin, X., Jiang, P., Ma, D., Li, M., 2019. Land system evolution of Qinghai-Tibetan Plateau under various development strategies. Appl. Geogr. 104, 1–9. https://doi.org/10.1016/j.apgeog.2019.01.007.

Li, X., Chen, G., Liu, X., Liang, X., Wang, S., Chen, Y., Pei, F., Xu, X., 2017. A new global land-use and land-cover change product at a 1-km resolution for 2010 to 2100 based on human–environment interactions. Ann. Assoc. Am. Geogr. 107 (5), 1040–1059. https://doi.org/10.1080/24694452.2017.1303357.

Li, H., Liu, Z., Lin, X., Qin, M., Ye, S., Gao, P., 2024. A novel spatiotemporal urban land change simulation model: Coupling transformer encoder, convolutional neural network, and cellular automata. J. Geogr. Sci. 34 (11), 2263–2287. https://doi.org/10.1007/s11442-024-2292-1.

Liang, X., Guan, Q., Clarke, K.C., Liu, S., Wang, B., Yao, Y., 2021. Understanding the drivers of sustainable land expansion using a patch-generating land use simulation (PLUS) model: a case study in Wuhan, China. Comput. Environ. Urban Syst. 85, 101569. https://doi.org/10.1016/j.compenvurbsys.2020.101569.

Lin, J., Li, X., Li, S., Wen, Y., 2020a. What is the influence of landscape metric selection on the calibration of land-use/cover simulation models? Environ. Model. Software 129, 104719. https://doi.org/10.1016/j.envsoft.2020.104719.

Lin, W., Sun, Y., Nijhuis, S., Wang, Z., 2020b. Scenario-based flood risk assessment for urbanizing deltas using future land-use simulation (FLUS): Guangzhou Metropolitan Area as a case study. Sci. Total Environ. 739, 139899. https://doi.org/10.1016/j.scitotenv.2020.139899.

Liu, C., Xu, Y., Huang, A., Liu, Y., Wang, H., Lu, L., Sun, P., Zheng, W., 2018. Spatial identification of land use multifunctionality at grid scale in farming-pastoral area: a case study of Zhangjiakou City, China. Habitat Int. 76, 48–61. https://doi.org/10.1016/j.habitatint.2018.05.010.

Liu, X., Liang, X., Li, X., Xu, X., Ou, J., Chen, Y., Li, S., Wang, S., Pei, F., 2017. A future land use simulation model (FLUS) for simulating multiple land use scenarios by coupling human and natural effects. Landsc. Urban Plann. 168, 94–116. https://doi.org/10.1016/j.landurbplan.2017.09.019.

Liu, Y., Dai, L., Long, H., 2023. Theories and practices of comprehensive land consolidation in promoting multifunctional land use. Habitat Int. 142, 102964. https://doi.org/10.1016/j.habitatint.2023.102964.

Lv, J., Song, C., Gao, Y., Ye, S., Gao, P., 2025. Simulation and analysis of the long-term impacts of 1.5°C global climate pledges on China's land systems. Sci. China Earth Sci. 68. https://doi.org/10.1007/s11430-023-1501-9.

Lv, J., Wang, Y., Liang, X., Yao, Y., Ma, T., Guan, Q., 2021. Simulating urban expansion by incorporating an integrated gravitational field model into a demand-driven random forest-cellular automata model. Cities 109, 103044. https://doi.org/10.1016/j.cities.2020.103044.

Peng, J., Liu, Y., Liu, Z., Yang, Y., 2017. Mapping spatial non-stationarity of human-natural factors associated with agricultural landscape multifunctionality in Beijing–Tianjin–Hebei region, China. Agric. Ecosyst. Environ. 246, 221–233. https://doi.org/10.1016/j.agee.2017.06.007.

Qian, F., Chi, Y., Lal, R., 2020a. Spatiotemporal characteristics analysis of multifunctional cultivated land: a case-study in Shenyang, Northeast China. Land Degrad. Dev. 31 (14), 1812–1822. https://doi.org/10.1002/ldr.3576.

Qian, Y., Xing, W., Guan, X., Yang, T., Wu, H., 2020b. Coupling cellular automata with area partitioning and spatiotemporal convolution for dynamic land use change simulation. Sci. Total Environ. 722, 137738. https://doi.org/10.1016/j.scitotenv.2020.137738.

Rallings, A.M., Smukler, S.M., Gergel, S.E., Mullinix, K., 2019. Towards multifunctional land use in an agricultural landscape: a trade-off and synergy analysis in the Lower Fraser Valley, Canada. Landsc. Urban Plann. 184, 88–100. https://doi.org/10.1016/j.landurbplan.2018.12.013.

Scherzinger, F., Schädler, M., Reitz, T., Yin, R., Auge, H., Merbach, I., Roscher, C., Harpole, W.S., Blagodatskaya, E., Siebert, J., 2024. Sustainable land management enhances ecological and economic multifunctionality under ambient and future climate. Nat. Commun. 15 (1), 4930. https://doi.org/10.1038/s41467-024-48830-z.

Schmid, M., Heinimann, A., Zaehringer, J.G., 2021. Patterns of land system change in a Southeast Asian biodiversity hotspot. Appl. Geogr. 126, 102380. https://doi.org/10.1016/j.apgeog.2020.102380.

van Asselen, S., Verburg, P.H., 2012. A land system representation for global assessments and land-use modeling. Global Change Biol. 18 (10), 3125–3148. https://doi.org/10.1111/j.1365-2486.2012.02759.x.

van Asselen, S., Verburg, P.H., 2013. Land cover change or land-use intensification: simulating land system change with a global-scale land change model. Global Change Biol. 19 (12), 3648–3667. https://doi.org/10.1111/gcb.12331.

van Vliet, J., Bregt, A.K., Hagen-Zanker, A., 2011. Revisiting Kappa to account for change in the accuracy assessment of land-use change models. Ecol. Model. 222 (8), 1367–1375. https://doi.org/10.1016/j.ecolmodel.2011.01.017.

Van Vliet, J., Verburg, P., 2018. A Short Presentation of CLUMondo, Geomatic Approaches for Modeling Land Change Scenarios. Springer, pp. 485–492.

Verburg, P.H., Soepboer, W., Veldkamp, A., Limpiada, R., Espaldon, V., Mastura, S.S., 2002. Modeling the spatial dynamics of regional land use: the CLUE-S model. Environ. Manag. 30 (3), 391–405. https://doi.org/10.1007/s00267-002-2630-x.

Vousdoukas, M.I., Athanasiou, P., Giardino, A., Mentaschi, L., Stocchino, A., Kopp, R.E., Menéndez, P., Beck, M.W., Ranasinghe, R., Feyen, L., 2023. Small Island Developing States under threat by rising seas even in a 1.5° C warming world. Nat. Sustain. 1–13. https://doi.org/10.1016/j.apgeog.2020.102380.

Vreeker, R., De Groot, H.L., Verhoef, E.T., 2004. Urban multifunctional land use: theoretical and empirical insights on economies of scale, scope and diversity. Built. Environ. 30 (4), 289–307. https://doi.org/10.2148/benv.30.4.289.57157.

Wang, C., Yu, C., Chen, T., Feng, Z., Hu, Y., Wu, K., 2020. Can the establishment of ecological security patterns improve ecological protection? An example of Nanchang, China. Sci. Total Environ. 740, 140051. https://doi.org/10.1016/j.scitotenv.2020.140051.

Wang, Y., Liu, Y., Chen, P., Song, J., Fu, B., 2024. Interannual precipitation variability dominates the growth of alpine grassland above-ground biomass at high elevations on the Tibetan Plateau. Sci. Total Environ. 931, 172745. https://doi.org/10.1016/j.scitotenv.2024.172745.

Wang, Y., Song, C., Gao, Y., Ye, S., Gao, P., 2024. Integrating national integrated assessment model and land-use intensity for estimating China's terrestrial ecosystem carbon storage. Appl. Geogr. 162, 103173. https://doi.org/10.1016/j.apgeog.2023.103173.

Xing, W., Qian, Y., Guan, X., Yang, T., Wu, H., 2020. A novel cellular automata model integrated with deep learning for dynamic spatio-temporal land use change simulation. Comput. Geosci. 137, 104430. https://doi.org/10.1016/j.cageo.2020.104430.

Zhai, Y., Yao, Y., Guan, Q., Liang, X., Li, X., Pan, Y., Yue, H., Yuan, Z., Zhou, J., 2020. Simulating urban land use change by integrating a convolutional neural network with vector-based cellular automata. Int. J. Geogr. Inf. Sci. 34 (7), 1475–1499. https://doi.org/10.1080/13658816.2020.1711915.

Zhang, T., Cheng, C., Wu, X., 2023. Mapping the spatial heterogeneity of global land use and land cover from 2020 to 2100 at a 1 km resolution. Sci. Data 10 (1), 748. https://doi.org/10.1038/s41597-023-02637-7.

Zhu, W., Gao, Y., Zhang, H., Liu, L., 2020. Optimization of the land use pattern in Horqin Sandy Land by using the CLUMondo model and Bayesian belief network. Sci. Total Environ. 739, 139929. https://doi.org/10.1016/j.scitotenv.2020.139929.